Modeling the Obstacle Performance of Cable-Towed Vehicles

Chengxian Gao[1]
Bruce Hartsough
John A. Miles
Andrew A. Frank
University of California, Davis, U.S.A.

ABSTRACT

The forces required to pull wheeled vehicles over idealized terrain obstacles were studied. Scale models and computer simulations were used to evaluate the peak forces for single-axle vehicles equipped with rigid wheels and pneumatic tires. A scale model of a rimless spoke wheel was also tested.

The results from the rigid wheel and pneumatic-tired simulations approximated those for the scale models. The rimless spoke wheel model required relatively high towing forces. The computer results indicated that towing forces could be reduced by a factor of three in some situations by using low pressure tires instead of rigid wheels. Even with low pressure tires, it is not possible to pull vehicles over obstacles larger than approximately 1/5 of the wheel diameter, if towing forces are not to exceed the vehicle weight.

Key Words: *tethered vehicles, simulation, timber harvesting, yarding*

Vehicles towed or tethered by cables have been suggested for various forest operations on steep slopes [5], [9], [10]. Tethered rollers were employed for site preparation in New Zealand [8] and one device was tested for yarding timber [2].
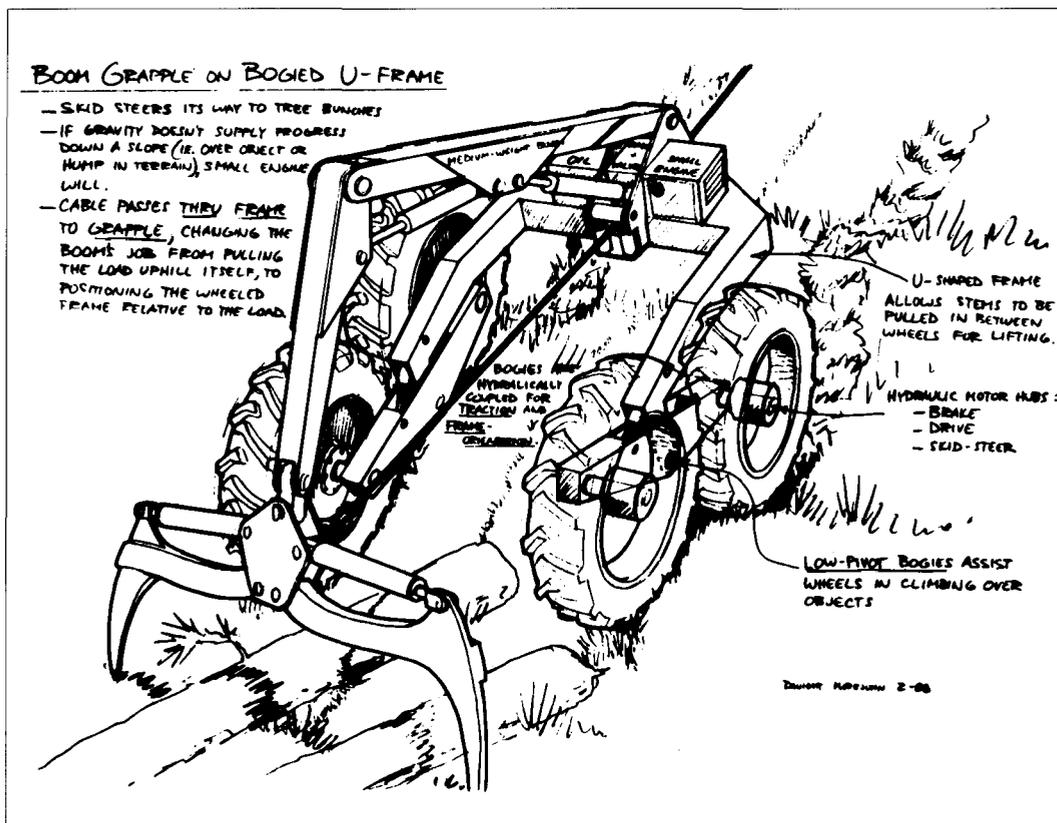

Figure 1. Cable-towed vehicle concept.

[1]*The authors are respectively: Staff Research Associate, Associate Professor and Professor, Agricultural Engineering Department; and Professor, Mechanical Engineering Department.*

Towed vehicles, represented by the concept shown in Figure 1, is investigated for transporting prebunched small timber on steep terrain. Earlier modeling work indicated that, when compared with
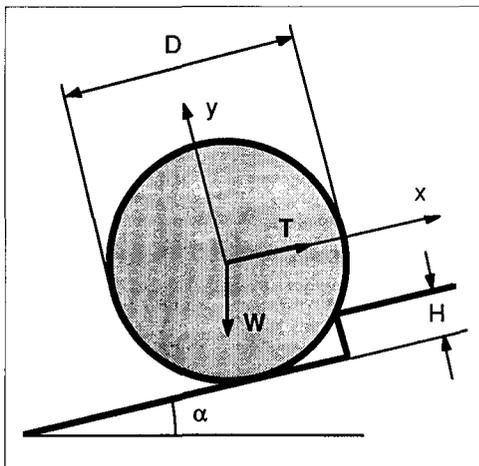
Figure 2. Obstacle and wheel geometry and forces.

conventional running skyline systems, cable-towed vehicles might reduce yarding costs by approximately 1/4, with greater reductions on less steep terrain and in areas with low deflection [4].

Obstacles, including stumps, slash, rocks and abrupt breaks in slope, would impede the travel of a towed vehicle. The size of osbstacles can be reduced, some can be completely removed by loggers, and others can be avoided by steering around them, but vehicles will have to traverse over some obstacles. To properly design a vehicle for logging, engineers must know how various vehicle configurations perform when traversing obstacles.

Previous research evaluated the obstacle performance of self-powered tractive vehicles. Bekker [1] theoretically investigated the abilities of two-axle vehicles to traverse obstacles, based on the assumptio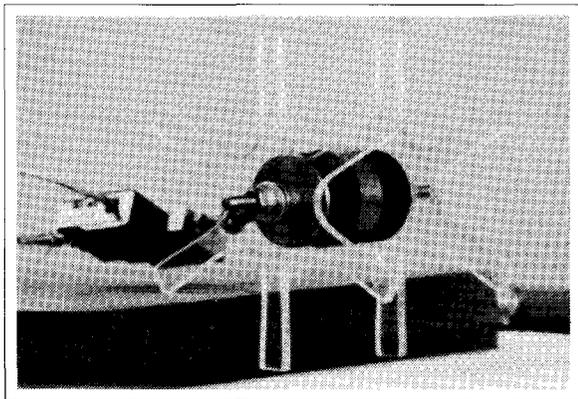ns of rigid wheels and rigid suspensions. He included obstacle height, wheel diameter and coefficient of adhesion as independent variables. His results indicated the largest obstacles that could be traversed by a given vehicle, assuming that torque was not limiting. Jindra [7] extended Bekker's study to permit the analysis of towed trailer effects on the obstacle performance of four-wheel drive vehicles, again using the assumption of rigid wheels. Janosi and Eilers [6] looked at the problem of hangups, where the vehicle frame bottoms out on the terrain. They only considered the geometry of the vehicle and the ground surface. None of these studies determined the forces required for towed vehicles, nor did they evaluate the effects of using low pressure pneumatic tires in place of rigid wheels. Since low-pressure tires are becoming more widely used in forestry applications and have apparent advantages when traversing obstacles, extension of the previous work to low pressure tires and other promising concepts is needed.

APPROACH

Computer simulation and scale models were used to study the towing forces required to pull the wheels of a single-axled vehicle over an idealized obstacle consisting of a right-angle step (Figure 2). Three types of wheels were considered: a) pneumatic-tired, b) a rimless, 6-spoke device which might "walk" over obstacles (Figure 3) and c) a rigid circular wheel as a standard for comparison.

Scale Models

Scale models were used for all three wheel types. Rigid and rimless spoke wheels of 6 inch diameter were fabricated from plexiglass, as were the step obstacles of various heights. Pneumatic inner tubes
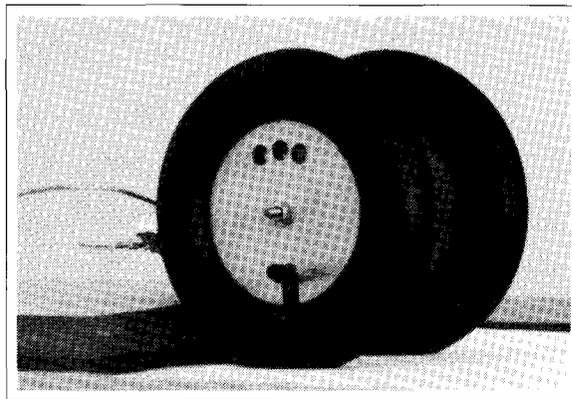

Figure 3. Scale model of vehicle equipped with rimless spoke wheels.

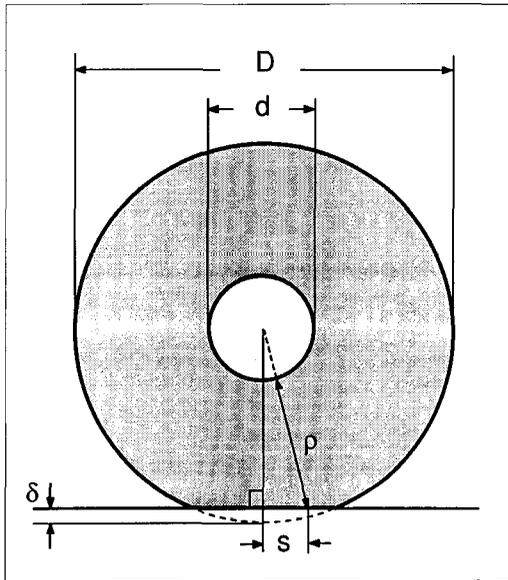**Figure 4.** Scale model of vehicle equipped with pneumatic tires.

Figure 5. Side view of deflected tire.

of 8 inch diameter were used as models for the pneumatic tires (Figure 4). The vehicles were towed by a variable-speed electric winch. Tension in the towing cable was monitored by an Interface SM-100 strain gage load cell placed between the cable and vehicle, while a string potentiometer measured the distance moved by the vehicle as it traversed the step. The data was recorded by a Campbell Scientific CR10 datalogger and downloaded to a microcomputer for analysis.

Computer Simulations

Computer simulations, based on theoretical static analysis, modeled vehicles with rigid and pneumatic tires. The analysis for rigid wheels was straightforward, resulting in a single relationship to estimate the peak towing force:

$$MAX\frac{T}{W} = \frac{2\sqrt{DH - H^2}}{D - 2H}\cos\alpha + \sin\alpha \qquad (1)$$

where
- T = towing force
- W = vertical load
- D = wheel diameter
- H = obstacle height
- α = ground slope.

The model for pneumatic tires was more complex. Figure 5 shows a side view of a deflected tire. It indicates how the deflected radial distance ρ is re-

lated to the deflection of the tire and position along the contact length with the surface (the ground or an obstacle):

$$\rho = \sqrt{\left(\frac{D}{2} - \delta\right)^2} - \frac{d}{2} \qquad (2)$$

where
- ρ = deflected radial distance between the rim and contact surface
- D = wheel diameter
- d = rim diameter
- δ = deflection of the tire, perpendicular to the contact surface
- s = distance along the contact surface from a radial plane perpendicular to the surface.

Initially, it was assumed that the tire had a rectangular cross section of constant width, even when deflected, which resulted in a surface contact area that was also rectangular. This model underestimated the towing forces.

The pneumatic tire model was reformulated, using the assumption that the tire wall had no resistance to bending and did not store energy. This gave, by minimum potential energy, a partial-circular cross section for the sidewall of the undeflected tire. When deflected, the sections of the sidewalls between the rim and the tire-ground contact surface were partial-circular, and the contact surface was tangent to the sidewalls (Figure 6). The radius of the deflected sidewall was related to the deflected distance ρ, and the rim and contact widths:
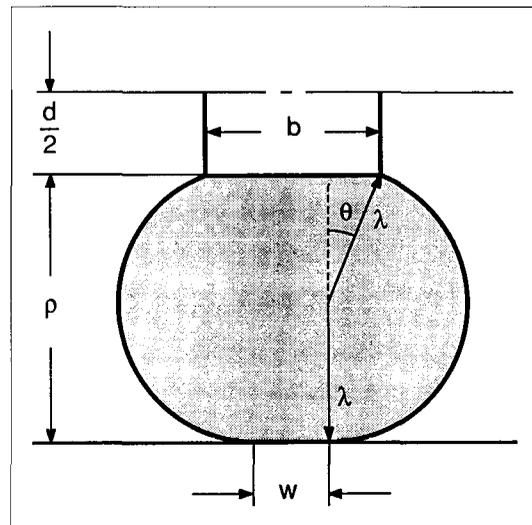

Figure 6. Radial cross section of deflected tire.

$$\lambda^2 = (\rho - \lambda)^2 + \left(\frac{b-w}{2}\right)^2 \qquad (3)$$

where

λ = radius of the deflected sidewall section
b = rim width
w = surface contact width.

This was rearranged to give:

$$2\lambda = \frac{\rho^2 + \left(\dfrac{b-w}{2}\right)^2}{\rho} \qquad (4)$$

The angle θ between the vertical plane and the rim-sidewall intersection was related to the surface contact width:

$$\theta = \sin^{-1}\left(\frac{b-w}{2\lambda}\right) \qquad (5)$$

and the partial-circular perimeter lengths plus the contact width must equal the fixed length c of the sidewall perimeter:

$$2\lambda(\pi - \theta) + w = c \qquad (6)$$

The sidewall perimeter length was determined by the specified values of wheel diameter D, width B of the undeflected sidewall section and rim width b:

$$c = \left(\pi - \sin^{-1}\left(\frac{b}{B}\right)\right)B \qquad (7)$$

Substituting (5) into (6) and rearranging gave a relationship between contact width w and sidewall section radius λ:

$$\sin\left(\frac{c-w}{2\lambda}\right) = \frac{b-w}{2\lambda} \qquad (8)$$

Combining (4) and (8) gave:

$$\sin\left(\frac{(c-w)\rho}{\rho^2 + \left(\dfrac{b-w}{2}\right)^2}\right) = \frac{(b-w)\rho}{\rho^2 + \left(\dfrac{b-w}{2}\right)^2} \qquad (9)$$

To be physically meaningful, ρ must be in the range 0 to $(D\text{-}d)/2$. Contact width w is bounded by 0 and $(b+c)/2$. For specified values of rim width b and sidewall perimeter c, the relationship between contact width w and radial distance ρ can be tabulated by solving (9) with an iterative root finding algorithm.

Assuming tire pressure remains constant regardless of tire deflection, the equilibrium equations derived with the principle of virtual work are:

$$p\frac{\partial V}{\partial x} = F_x \qquad (10)$$

and

$$p\frac{\partial V}{\partial y} = F_y \qquad (11)$$

where

p = tire inflation pressure
V = tire volume
x = displacement of the axle, parallel to the ground, with respect to the position when the undeflected tire is just contacting the step obstacle
y = displacement of the axle, perpendicular to the ground, up with respect to the undeflected position
F_x, F_y = the forces, other than contact forces normal to the surfaces, exerted on the wheel along the x and y directions respectively. F_x includes the towing force and the component of vertical load parallel to the ground; F_y consists of the vertical load component perpendicular to the ground.

The partial derivatives of tire volume are the projected contact areas A_x and A_y perpendicular to the x and y directions respectively, so the equilibrium relationships become:

$$pA_x = F_x \qquad (12)$$

and

$$pA_y = F_y \qquad (13)$$
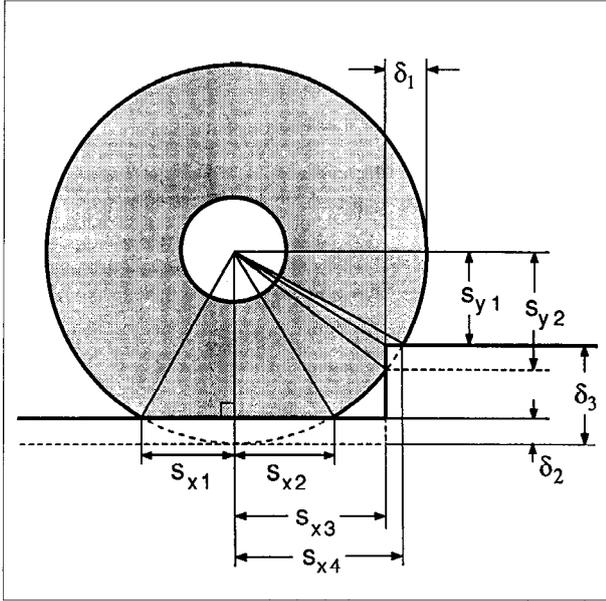
For the step obstacle, the projected areas are:

Figure 7. Deflections and integration limits.

$$A_x = \int_{s_{y1}}^{s_{y2}} w(s_1 \delta_1) ds \qquad (14)$$

and

$$A_y = \int_{s_{x1}}^{s_{x2}} w(s_1 \delta_2) ds + \int_{s_{x3}}^{s_{x4}} w(s_1 \delta_3) ds \qquad (15)$$

where δ_1, δ_2, and δ_3 are the deflections correspond-ing to the three subareas (see Figure 7), and the contact surface width $w(s,\delta)$ is determined as an implicit function of s and δ by combining equations (2) and (9). The deflections are:

$$\delta_1 = x + \left(\frac{D}{2} - L \right) \qquad (16)$$

$$\delta_2 = -y \qquad (17)$$

$$\delta_3 = y + H \qquad (18)$$

where
H = the obstacle height
L = the distance in the x direction of the obstacle in front of the axle when the undeflected tire is just contacting the obstacle. This distance is given by:

$$L = \sqrt{\left(\frac{D}{2} \right)^2 - \left(\frac{D}{2} - H \right)^2} \qquad (19)$$

The limits of the integrals are calculated as follows:

$$s_{y1} = \frac{D}{2} + y - H \qquad (20)$$

$$s_{y2} = \min\left(\sqrt{\left(\frac{D}{2} \right)^2 - (L - x)^2}, \frac{D}{2} + y \right) \qquad (21)$$

$$s_{x1} = -\sqrt{\left(\frac{D}{2} \right)^2 - \left(\frac{D}{2} + y \right)^2} \qquad (22)$$

$$s_{x2} = \min(-s_{x1}, L - x) \qquad (23)$$

$$s_{x3} = L - x \qquad (24)$$

$$s_{x4} = \sqrt{\left(\frac{D}{2} \right)^2 - \left(\frac{D}{2} + y - H \right)^2} \qquad (25)$$

Using equation (2) and a tabulated relationship be-tween w and ρ obtained from solving equation (9), equations (14) and (15) can be evaluated numerically using Gauss-Legendre N-point integration [3].

A computer simulation program, using the mathematical model developed above, was imple-mented to simulate the process of a pneumatic-tired wheel traversing a step obstacle. The general flow of the simulation was as follows:

The user input the dimensions of the wheel and vertical load, inflation pressure, obstacle height and ground slope. The program then generated two lookup tables, one for the values of the N points and corresponding weights for the Gauss-Legendre inte-gration rule, the other tabulating the w-ρ relation-

ship in equation (9). The golden section method [11] was found to be successful for finding the corresponding root w at each given p.

Starting from the initial position where the wheel just contacted the obstacle, the wheel was moved in incremental distance steps in the x direction. At each step the program searched, using equation (13) and the golden section method, for the equilibrium y coordinate. The search involved a series of evaluations of equation (15) to find the contact area A_y. After the y coordinate was found, equations (14) and (12) were solved to give A_x, then F_x, from which the towing force T was calculated. At each step in the x direction, the program output the displacement x, the equilibrium value of y and the towing force T. The simulation was terminated when the wheel axle reached the top of the step obstacle.

The terrain and wheel parameters were combined into seven dimensionless ratios. The five independent ratios were:

SLOPE   ground slope in percent
H/D   obstacle height : wheel diameter ratio
W/pBD   tire flexure index (zero for rigid wheels)
x/D   travel distance : wheel diameter ratio
b/B   rim width : wheel width ratio
d/D   rim diameter : wheel diameter ratio

and the dependent variables were:

T/W   towing force : vertical load ratio
MAX T/W   the peak value of T/W as the wheel traverses the obstacle.
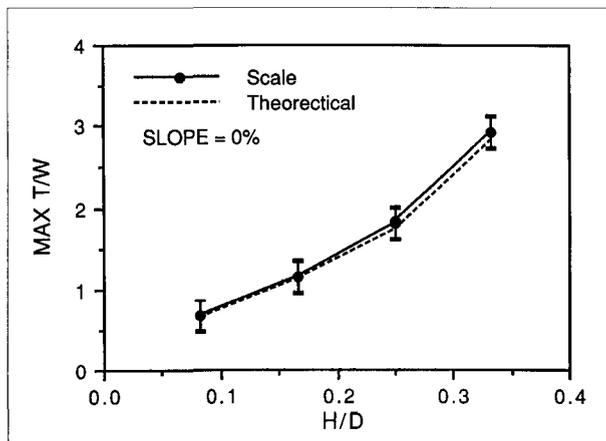
The performance of wheel configurations were compared for various values of H/D, W/pBD and SLOPE. The ratio b/B was fixed at 0.429 (= 0.75"/1.75"), and the ratio d/D was fixed for given D, B and b such that the sidewall of the undeflected tire was shaped partial-circular.

RESULTS

For rigid wheels the scale model gave results which closely approximated those from theory (Figure 8).

For pneumatic tires, the computer and scale models did not agree as closely. Examples of force versus displacement traces are shown in Figure 9, and maximum towing force results are displayed in Figure 10. In most situations, the scale model indicated a higher towing force than did the computer simulation for a given set of conditions. These differences are probably due to the rolling resistance and carcass stiffness of the model tire.

The computer model was used to compare rigid wheels and pneumatic tires over a wide range of conditions (Figures 11 and 12). The computer model predicted that use of a relatively soft tire (W/pBD = 0.3) would reduce towing force requirements drastically (e.g. by 70 percent for H/D = 0.4 and SLOPE = 0 percent) when compared to those for a rigid wheel of equal diameter.

The model showed that the rimless spoke wheel was able to traverse obstacles that were theoretically not possible to climb with a rigid wheel, but towing
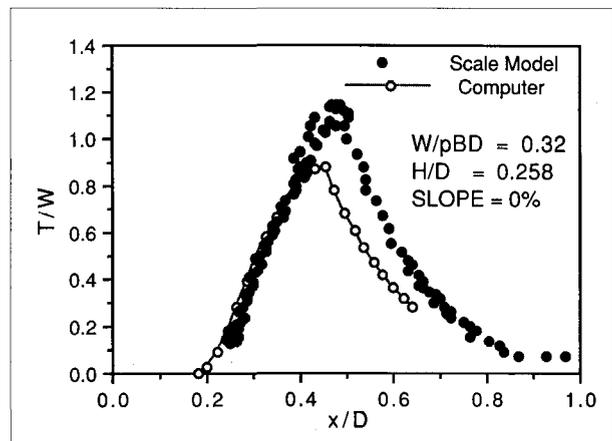

Figure 8. Comparison of maximum towing forces for a vehicle with rigid wheels, theoretical versus scale model.

Figure 9. Comparison of towing force traces for a vehicle with pneumatic tires, computer simulation versus scale model.
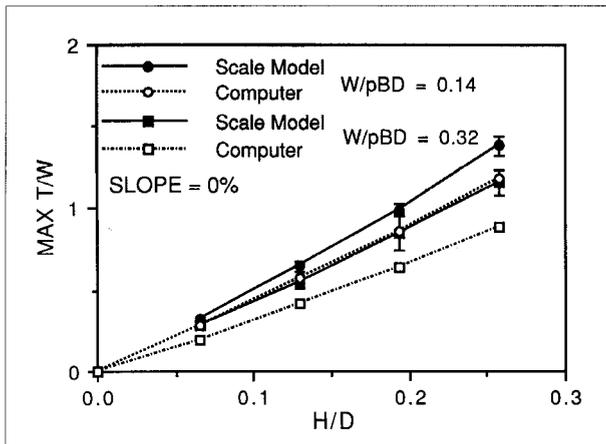
Figure 10. Comparison of maximum towing force results for a vehicle with pneumatic tires, computer simulation versus scale model.
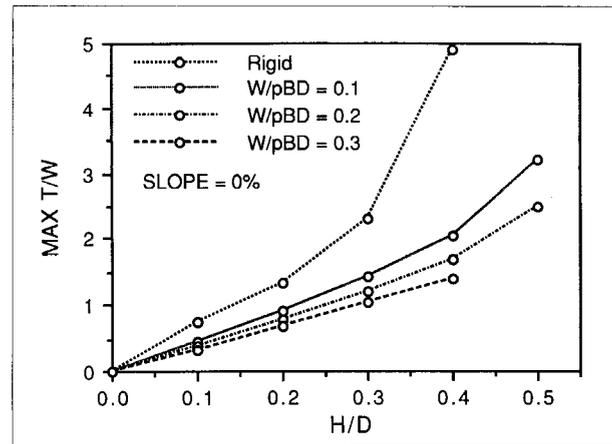

Figure 11. Maximum towing force results from computer simulation for a vehicle with pneumatic tires, with slope = 0 percent.

force requirements were relatively high for small obstacles and even on flat ground (Figure 13). This was due to the climbing motion of the wheel after each spoke contacted the ground.

CONCLUSIONS

The work by Gao and Hartsough [4] showed that, for a cable-towed vehicle to be economically practical, the towed force to weight ratio should not exceed approximately 1, although the maximum feasible value depends on the specific conditions and how they affect the economics of the alternative cable systems. To keep towing force less than or

equal to the vehicle weight, the results of this study indicate that a vehicle with rigid wheels operating on a 50 percent slope can traverse an obstacle no larger than 1/10 of the wheel diameter. The ratio of H/D can be no larger than 1/10 for a rimless spoke wheel, even on flat ground. The computer model indicated that a low pressure tire (W/pBD = 0.3) can operate on a 50 percent slope with an H/D of up to 1/5, so pneumatic tires are clearly advantageous for cable-towed vehicles. Avoiding larger obstacles, either by removing them or by steering around them, appears to be critical for practical operation. Supplying torque to the wheels would reduce the pull requirements, but overuse of tractive power could result in excessive soil disturbance.
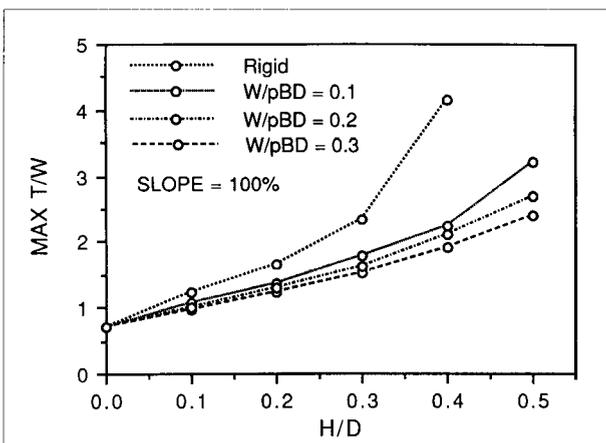

Figure 12. Maximum towing force results from computer simulation for a vehicle with pneumatic tires, with slope = 100 percent.
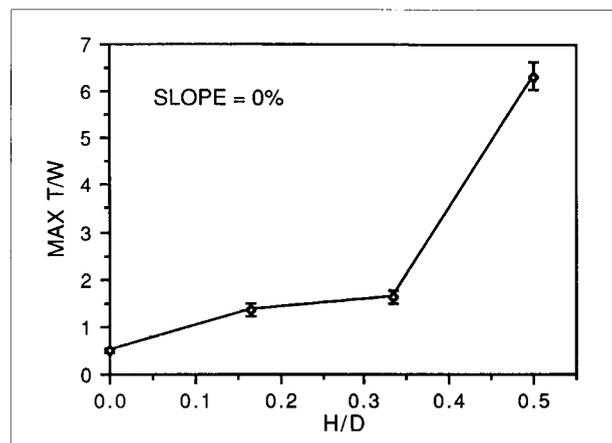

Figure 13. Maximum towing force results from scale modeling for a vehicle with rimless spoke wheels, with slope = 0 percent.

ACKNOWLEDGEMENT

LITERATURE CITED

[1]   Bekker, M.G. 1956. Theory of land locomotion. University of Michigan Press, Ann Arbor. 522p.

[2]   Biller, C.J. and H.G. Gibson. 1978. Testing the Chuball for selective logging on Appalachian slopes. Northern Logger and Timber Processor, June. p. 18,19,34.

[3]   Davis, P.J. and P. Robinnowitz. 1975. Methods of Numerical Integration. Academic Press, New York. 459p.

[4]   Gao, C. and B.R. Hartsough. 1988. Concepts for harvesting timber on steep terrain. Transactions of the ASAE 31(2):362-368.

[5]   Gonsier, M.J. 1980. A new concept for using the unusable. IN: Land-Use Allocation: Processes, People, Politics, Professionals., Proceedings of the 1980 Convention of The Society of American Foresters. p. 289-293.

[6]   Janosi, Z.J. and J.A. Eilers. 1968. Analysis of the basic curve of obstacle negotiation. J. of Terramechanics 5(3):29-42.

[7]   Jindra, F. 1966. Obstacle performance of articulated wheeled vehicles. J. of Terramechanics 3(2):39-56.

[8]   Larson, J. and R. Hallman. 1980. Equipment for reforestation and timber stand improvement. U.S. Forest Service, Equipment Development Center, Missoula, MT. p. 15-16.

[9]   McKenzie, D.W. and B.Y. Richardson. 1978. Feasibility study of self-contained tether cable system for operating on slopes of 20 to 75%. J. of Terramechanics 15(3):113-127.

[10]   Schenk, R.B. 1968. Cable logging system. U.S. Patent No. 3,390,863. July 2.

[11]   Vanderplaats, G.N. 1984. Numerical Optimization Techniques for Engineering Design with Applications. McGraw-Hill Book Company, New York. 333p.